GBE

Structural Rearrangements and Selection Promote Phenotypic Evolution in *Anolis* Lizards

Raúl Araya-Donoso [1], Sarah M. Baty [1], Jaime E. Johnson [1], Eris Lasku[1], Jody M. Taft [2], Rebecca E. Fisher [1], Jonathan B. Losos [3], Greer A. Dolby [4], Kenro Kusumi [1], Anthony J. Geneva [2,*]

[1]School of Life Sciences, Arizona State University, Tempe, AZ 85287, USA

[2]Department of Biology & Center for Computational and Integrative Biology, Rutgers University–Camden, Camden, NJ 08103, USA

[3]Department of Biology, Washington University, Saint Louis, MO, USA

[4]Department of Biology, University of Alabama, Birmingham, AB, USA

*Corresponding author: E-mail: anthony.geneva@rutgers.edu.

Accepted: October 09, 2025

Abstract

The genomic characteristics of adaptively radiated groups could contribute to their high species number and ecological disparity, by increasing their evolutionary potential. Here, we explored the genomic variation of *Anolis* lizards, focusing on three species with distinct phenotypes: *Anolis auratus*, one of the species with the longest tail; *Anolis frenatus*, one of the largest species; and *Anolis carolinensis*, one of the species that inhabits the coldest environments. We assembled and annotated two new chromosome-level reference genomes for *A. auratus* and *A. frenatus* and compared them with the available genomes of *A. carolinensis* and *Anolis sagrei*. We evaluated the presence of structural rearrangements, quantified the density of repeat elements, and identified potential signatures of positive selection in coding and regulatory regions. We detected substantial rearrangements in scaffolds 1, 2, and 3 of *A. frenatus* different from the other species, in which the rearrangement breakpoints corresponded to hotspots of developmental genes. Further, we detected an accumulation of repeats around key developmental genes in anoles and phrynosomatid outgroups. Finally, coding sequences and regulatory regions of genes relevant to development and physiology showed variation that could be associated with the unique phenotypes of the analyzed species. Our results show examples of the hierarchical genomic variation within anoles that could provide the substrate that promoted phenotypic disparity and contributed to their adaptive radiation.

Key words: adaptive radiation, comparative genomics, reference genome, transposable elements.

Significance

In this study, we generated high-quality reference genome assemblies and annotations for two species of anole lizards. Our analyses show examples of some genomic characteristics within the *Anolis* adaptive radiation that could be associated with the high diversity found in the genus. These genomes are valuable resources for comparative genomics and evolutionary biology research, as they can aid future research efforts to link the genomic variation of organisms with their evolutionary potential.

© The Author(s) 2025. Published by Oxford University Press on behalf of Society for Molecular Biology and Evolution.
This is an Open Access article distributed under the terms of the Creative Commons Attribution-NonCommercial License (https://creativecommons.org/licenses/by-nc/4.0/), which permits non-commercial re-use, distribution, and reproduction in any medium, provided the original work is properly cited. For commercial re-use, please contact reprints@oup.com for reprints and translation rights for reprints. All other permissions can be obtained through our RightsLink service via the Permissions link on the article page on our site—for further information please contact journals.permissions@oup.com.

Downloaded from https://academic.oup.com/gbe/article/17/11/evaf196/8303492 by guest on 27 January 2026

Introduction

Adaptively radiated groups of organisms are natural experiments in which the relative roles of ecological and genomic factors on speciation and phenotypic differentiation can be assessed (Schluter 2000; Martin and Richards 2019; Gillespie et al. 2020). In general, ecological variation and the emergence of ecological opportunity are known to play an important role in determining the ability of a group of organisms to radiate adaptively (Wellborn and Langerhans 2015; Stroud and Losos 2016). On the other hand, genetic mechanisms could also influence the ability of organisms within radiations to diversify and generate extensive phenotypic variation because clades with greater evolutionary potential could be more likely to radiate adaptively (Seehausen et al. 2014; Gillespie et al. 2020). Multiple genetic mechanisms could contribute to increased genetic and phenotypic diversity such as chromosome-level structural rearrangements, small-scale structural variation, the dynamics of transposable elements (TEs), mutation rates, recombination rates, and the genomic landscape of selection on regulatory elements and/or coding regions (Brawand et al. 2014; Seehausen et al. 2014; Han et al. 2017; Bourque et al. 2018; Mérot et al. 2020).

The relevance of the genomic substrate for highly speciose or adaptively radiated groups of organisms has been discussed before. For example, African lake cichlids show ancient genetic polymorphisms, structural rearrangements, high divergence in regulatory sequences, insertion of transposable elements within regulatory elements, and novel microRNAs (miRNAs) (Brawand et al. 2014; Seehausen et al. 2014; McGee et al. 2020). Darwin's finches also exhibit evidence of ancient polymorphisms, and selection on large-effect loci associated with beak morphology located in genomic islands of low recombination (Han et al. 2017; Rubin et al. 2022). *Heliconius* butterflies present increased genomic variation by hybridization and/or introgression processes, high variability in regulatory regions, genome expansion events caused by an increase in repeat elements, and structural rearrangements (Edelman et al. 2019; Lewis and Reed 2019; Kozak et al. 2021; Seixas et al. 2021). Therefore, groups that radiate could have more labile genomes that allow for greater phenotypic diversification. A current challenge is to determine the relative importance of each of these genomic factors and whether different radiations present similar genomic variation that aided diversification or whether different radiations have occurred through different genomic mechanisms.

Anolis lizards are an ideal group to assess the relevance of genetic mechanisms for generating and promoting phenotypic diversity. This genus is described as an adaptive radiation with ~400 species distributed in the tropical Americas (Losos 2011; Muñoz et al. 2023). *Anolis* are considered a model system for evolutionary biology studies because they present extensive phenotypic variation across multiple niche axes. A remarkable characteristic of *Anolis* evolution is the repeated occurrence of intra-island radiation and morphological differentiation associated with microhabitat use patterns (Losos 1990; Mahler et al. 2010; Huie et al. 2021). Besides morphology, anoles have diversified in behavior, physiology, and sexual dimorphism (Butler et al. 2007; Velasco et al. 2016; Gunderson et al. 2018). In this context, anoles present a wide range of phenotypic variation compared to other taxa, and this diversity may be promoted by ecological and genetic mechanisms.

Within the *Anolis* radiation, some species have disparate phenotypes that could be adaptive to their niches (Fig. 1a). We focused on body size, tail length (TL), and cold tolerance as ecologically meaningful traits with high variation within *Anolis* (Mahler et al. 2010, Table S1), and particularly variable among the *Anolis* species with genome assemblies available. For example, *A. frenatus* is among the larger anole species (Fig. 1b), which may reduce its predation risk and enable a wider dietary breadth, potentially including other anole lizards as prey (Losos et al. 1991); *Anolis auratus* inhabits grasslands and perches on narrow branches and features an extremely long tail (Fig. 1c), a trait that may provide better balance in species that walk and jump along narrow surfaces (Gillis et al. 2009; Hsieh 2015); and *Anolis carolinensis* is one of the species with the highest cold tolerance (Fig. 1d), enabling its colonization in higher latitudes and survival during cold seasons (Campbell-Staton et al. 2018). Different types of genomic variation, particularly within coding regions, may control such traits. For instance, longer tails could be produced by modifications of the number and/or size of the caudal vertebrae, controlled by molecular pathways involved in the axial skeleton development (Mallo 2018, 2020; Bergmann and Morinaga 2019). A larger body size could be controlled by insulin growth factor or growth hormone pathways (Rotwein 2018; Beatty and Schwartz 2020; Duncan et al. 2020), while cold adaptation could be related to genes regulating oxygen consumption and/or blood circulation (Pörtner 2001; Campbell-Staton et al. 2018).

A variety of genomic characteristics have been hypothesized to play a role in the great ecological disparity observed among *Anolis* species. Tollis et al. (2018) compared short-read genome assemblies of five species (including *A. carolinensis*, *A. auratus*, and *Anolis frenatus*) and detected high mutation rates in anoles compared to other vertebrates and signatures of natural selection on genes associated with limb and brain development and hormonal regulation. In some Cuban anole species, an accumulation of gene duplications has been reported (Kanamori et al. 2022), and genomic regions undergoing accelerated evolution have been identified in association with thermal biology (Sakamoto et al. 2024). Furthermore, *Anolis* genetic diversity could have been fueled by ancient hybridization and introgression processes (Farleigh et al. 2023; Wogan et al. 2023).

Downloaded from https://academic.oup.com/gbe/article/17/11/evaf196/8303492 by guest on 27 January 2026

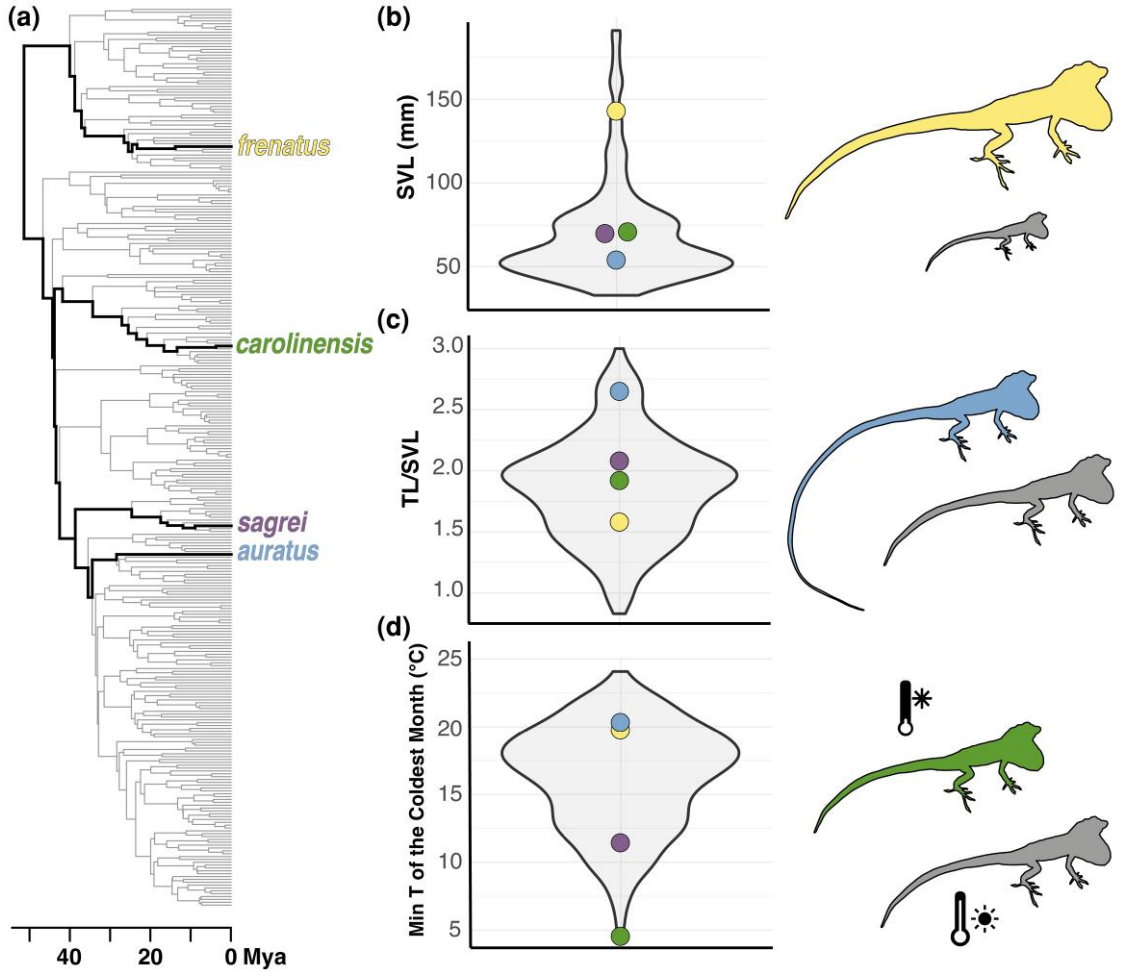

Fig. 1. *Anolis* phylogenetic relationships (a) and genus-wide phenotypic variation in snout–vent length (SVL; b), tail length (TL; c), and thermal climatic niche (d), highlighting the species included in this study (phylogenetic and morphological data from Poe et al. 2017; temperature data obtained from WorldClim 2, Fick and Hijmans 2017, for all species).

Chromosomal rearrangements could also be relevant because multiple events of chromosome gains and losses have been described within *Anolis* (Castiglia et al. 2013; Gamble et al. 2014), and chromosome fission and fusions have been proposed to determine the evolution of the *Anolis* X chromosome (Giovannotti et al. 2017; Geneva et al. 2022). Finally, the dynamics of repeat elements could be relevant because transposable elements can impact the genome by modifying gene regulation patterns, causing mutations or promoting genome rearrangements (Bourque et al. 2018). A high density of transposable elements within the *hoxB* and *hoxC* gene clusters, key regulators of morphological development, has been reported in *Anolis* (Di-Poï et al. 2010; Feiner 2016, 2019). Nonetheless, genome-wide patterns associated with repeat density and structural rearrangements remain to be explored with chromosome-level genome assemblies.

Here, we explored the genomic variation of species with disparate phenotypes within the adaptively radiated *Anolis* group. We generated chromosome-level reference genomes for two *Anolis* species and found evidence for major structural rearrangements, described a unique pattern of repeat density through the genome, and identified genes putatively under positive selection. We hypothesize that this variation could influence the unique traits of four species representing divergent phenotypes. By analyzing a subset of the anole radiation, these results show an example of the potentially diverse genomic architecture within *Anolis*, which could fuel genetic diversity and hence promote high diversification and phenotypic disparity in the genus.

Results

Chromosome-Level Genome Assemblies and Annotation for *A. auratus* and *A. frenatus*

We generated chromosome-level genome assemblies for two *Anolis* species (Table 1). Both type specimens were adult females from Panama (Table S2). The total sequencing coverage

Downloaded from https://academic.oup.com/gbe/article/17/11/evaf196/8303492 by guest on 27 January 2026

Table 1 Genome assembly and annotation statistics for the four analyzed *Anolis* species

Species	*A. auratus*	*A. frenatus*	*A. carolinensis*	*A. sagrei*
Genome version	RUC_Aaur_2	RUC_Afre_2	AnoCar2.0	AnoSag2.1
Assembly length (Gb)	1.77	1.85	1.79	1.66
N50 (Mb)	281.8	342.7	150.6	253.6
L50 (no.)	3	3	5	4
Eukaryote BUSCO assembly (%)	C + F: 93.07	C + F: 86.14	C + F: 94.5	C + F: 100
% repeats	48.53	51.27	33	46.3
No. genes	19,879	19,643	21,555	20,033
Average gene length (bp)	19,877	18,033	32,969	45,059
Eukaryote BUSCO annotation (%)	C + F: 88.2	C + F: 76.1	C + F: 94.5	C + F: 99.7
Reference	This study	This study	Alföldi et al. (2011)	Geneva et al. (2022)

was 259× (116× short reads, 70× Chicago, and 73× Hi-C) for *A. auratus* and 370× (105× short reads, 128× Chicago, and 137× Hi-C) for *A. frenatus*. The resulting assemblies were contiguous (*A. auratus*: 281.8 Mb of N50 and 0.916% gap; *A. frenatus*: 342.7 Mb of N50 and 1.464% gap) and moderately complete (BUSCO eukaryotic completeness of 93.07% for *A. auratus* and 86.14% for *A. frenatus*). The percentage of missing genes could be attributed to highly fragmented contigs in the assemblies (contig N50: *A. auratus* 18.64 kb; *A. frenatus* 10.19 bp). Both species show a similar pattern of repetitive element composition (Fig. S1), which corresponds to roughly 50% of the genome. However, *A. auratus* shows a recent accumulation of long interspersed nuclear elements (LINEs). We generated genome annotations for both species via the MAKER pipeline (Campbell et al. 2014) using a combination of new data and the proteomes of previously sequenced species (see Methods for details). For *A. auratus*, we identified 19,879 genes with an average length of 19,877 bp (Table 1, Table S3), and 88.2% of all eukaryote benchmarking universal single-copy ortholog (BUSCO) genes present in the annotation (either complete or fragmented), whereas for *A. frenatus*, 19,643 genes were identified with an average length of 18,033 bp (Tables 1 and S3) and 76.1% eukaryotic BUSCO genes present. For subsequent analyses, our newly annotated genomes were compared against the chromosome-level reference genomes of *A. carolinensis* (AnoCar2.0, Alföldi et al. 2011; and DNAzoo Hi-C Assembly, Dudchenko et al. 2017, 2018) and *Anolis sagrei* (AnoSag2.1, Geneva et al. 2022), along with the phrynosomatid lizards *Urosaurus nigricaudus* (Davalos-Dehullu et al. 2023) and *Phrynosoma platyrhinos* (Koochekian et al. 2022).

Chromosome-Level Structural Rearrangements

We performed in silico chromosome painting to assess the synteny conservation among our four *Anolis* species and *U. nigricaudus* and *P. platyrhinos*, using *A. sagrei* as a reference. Overall, there is high synteny conservation for the main scaffolds or macrochromosomes among those species (Fig. 2a). Interestingly, scaffolds 1, 2, and 3 contain substantial structural rearrangements that are unique to *A. frenatus* (Fig. 2a and b). The Hi-C data for *A. frenatus* show higher contact density within scaffolds and very little interaction between scaffolds 1, 2, and 3 (Figs. 2c and S2). This observation suggests that the observed rearrangements are not a sequencing or scaffolding artifact but rather support genuine structural differences in this species relative to other Iguanian taxa.

Structural rearrangements can modify the gene regulation and affect recombination patterns (Mérot et al. 2020; Damas et al. 2021). Therefore, we identified the genes located within 1 Mb of the rearrangement breakpoints in scaffolds 1, 2, and 3 between *A. sagrei* and *A. frenatus* (Table S4) to hypothesize functional implications of this mutation. We conducted an enrichment analysis on the list of genes colocated with the breakpoints using g:Profiler (Kolberg et al. 2023), which showed significant enrichment of biological processes such as "cellular differentiation," "developmental process," and "pigment granule transport" (Table S5). Further, we quantified the density of genes associated with developmental gene ontology (GO) terms along scaffolds 1, 2, and 3 of *A. frenatus*, and we detected that the chromosomal breaks were located in hotspots of genes with developmental functions (Fig. 2d). Among the genes contiguous to the rearrangement breakpoints (Table S4), we identified *axin2*, a regulator of the Wnt/β-catenin and TGF-β pathways that determines chondrocyte maturation and axial skeletal development (Dao et al. 2010); *bmp2*, a growth factor determinant for bone development through the BMP-Smad pathway (Shu et al. 2011); *ddit3*, a transcription factor that influences myogenesis by regulating the GH-IGF1 pathway (Zecchini et al. 2019); and *twist2*, a transcription factor relevant for bone formation and myogenesis (Liu et al. 2017).

Scaffold 7 in *A. sagrei* has previously been hypothesized to be the X chromosome and the result of a series of autosomal fusions (Kichigin et al. 2016; Giovannotti et al. 2017; Geneva et al. 2022). *A. auratus* and *A. sagrei* belong to the *Norops* clade of *Anolis* (Poe et al. 2017). We found a high degree of synteny conservation between the scaffold 7 of these two species, whereas in the species outside of the *Norops* clade, it corresponded to a series of smaller scaffolds (Figs. 2a and S3). To further explore scaffold 7

Downloaded from https://academic.oup.com/gbe/article/17/11/evaf196/8303492 by guest on 27 January 2026

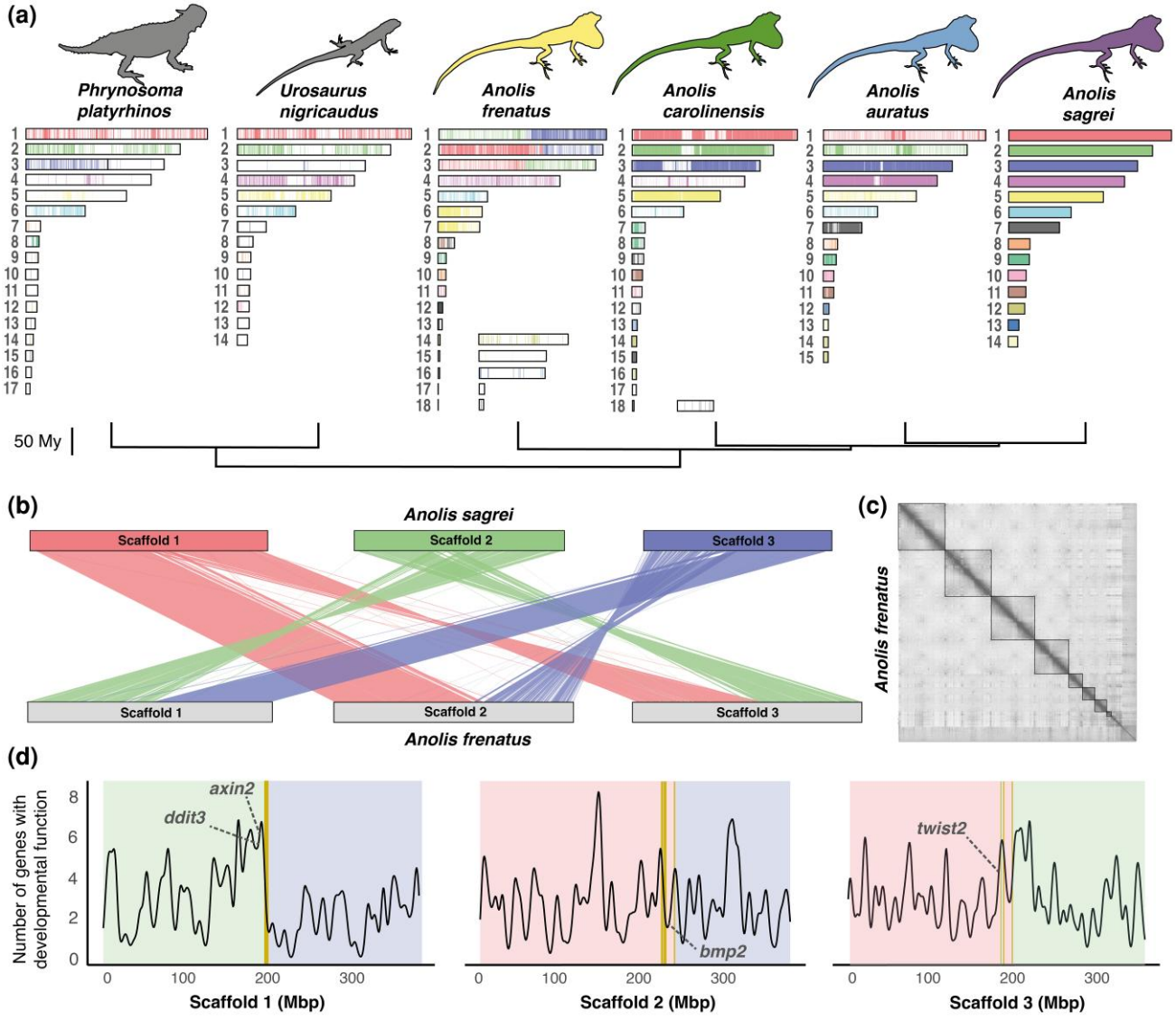

Fig. 2. Chromosome-level structural variation across *Anolis*. a) Synteny between *A. sagrei* and other anole (*A. auratus*, *A. carolinensis*, *A. frenatus*) and lizard (*U. nigricaudus*, *P. platyrhinos*) species for the largest scaffolds representing the chromosomes of each species. b) Synteny between scaffolds 1, 2, and 3 of *A. sagrei* and *A. frenatus* showing substantial rearrangements. c) Hi-C density contact matrix for *A. frenatus*. d) Density of genes associated with developmental GO terms along scaffolds 1, 2, and 3 in *A. frenatus*. Background colors indicate the homology to *A. sagrei* scaffolds for different chromosomal regions, and vertical lines indicate the chromosomal breakpoints. Rearrangement breakpoints are within hotspots of developmental genes.

evolution within anoles, we compared this chromosome against another recently published *Norops* clade high-quality genome, *Anolis apletophallus* (Pirani et al. 2023), which also revealed high synteny conservation with both *A. sagrei* and *A. auratus* (Fig. S3).

Repeat Density Is Associated With Key Developmental Genes in *Anolis* and Other Pleurodonts

The relative composition of repeat elements differed among species, as anoles have a higher proportion of DNA transposons and LINEs, whereas phrynosomatids have a relatively higher proportion of long terminal repeats (Table S6; Fig. S4). We estimated the density of repeats in 500-kb windows throughout the first six scaffolds of *A. frenatus*, *A. auratus*, *A. sagrei*, *U. nigricaudus*, and *P. platyrhinos*. We selected the densest repeat regions corresponding to the top 5% of repeat density and identified the genes present in those regions from our annotations (Table S7). For all species, the composition of repeats within repeat-rich regions did not differ significantly from the relative abundance of repeat elements in scaffolds 1 through 6 (Table S6). Within these regions, in all the analyzed species, we detected some developmental genes (Fig. 3) such as the

Downloaded from https://academic.oup.com/gbe/article/17/11/evaf196/8303492 by guest on 27 January 2026

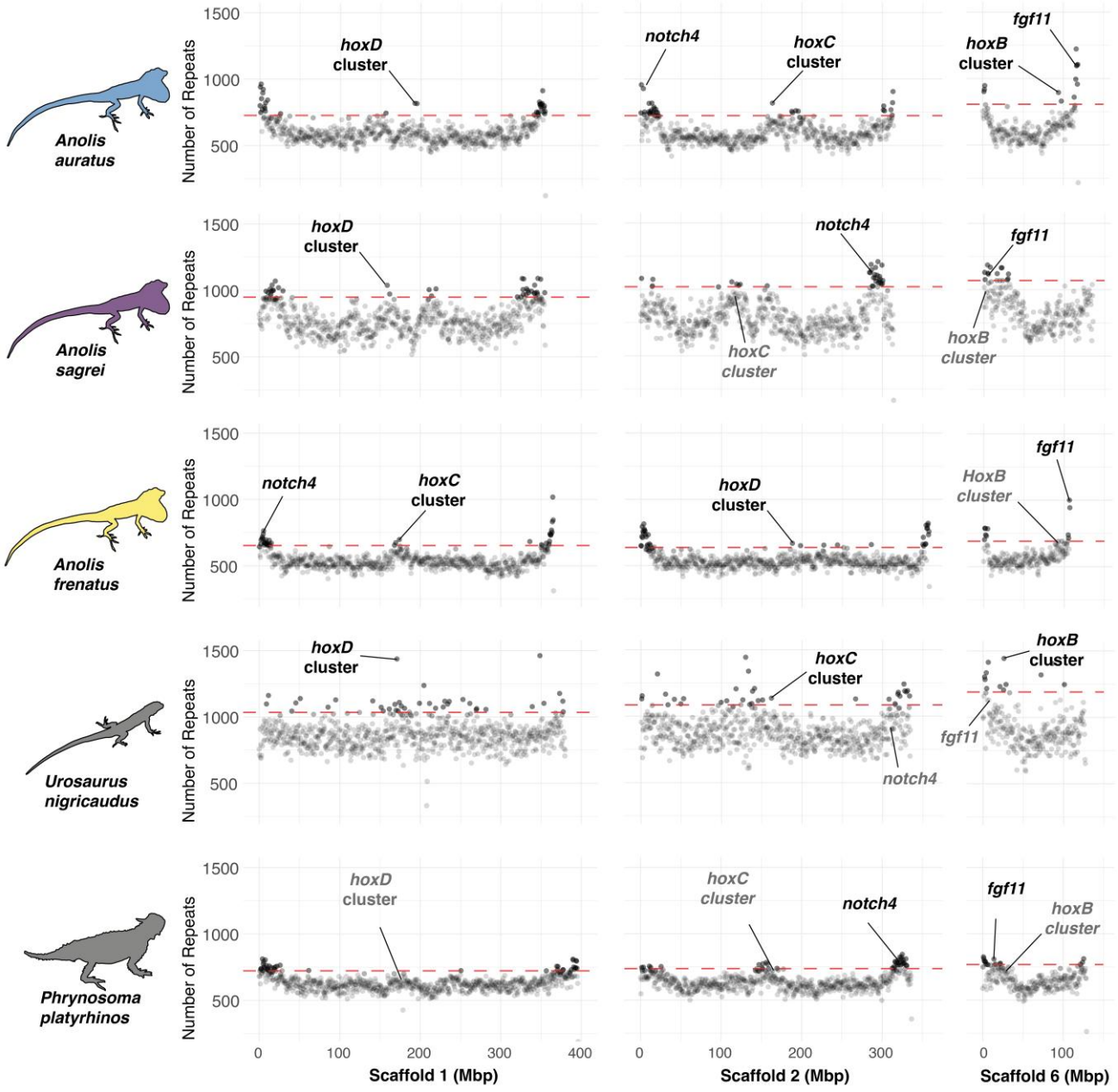

Fig. 3. Number of repeat elements in 500-kb windows throughout scaffolds 1, 2, and 6 in the analyzed pleurodont species. A higher density of repeats is found close to key developmental genes in the four *Anolis* and the outgroups.

hoxB, *hoxC*, and *hoxD* gene clusters, key determinants of the vertebrate body plan (Mallo 2018); *notch4*, a member of the NOTCH receptor family that is crucial for development (James et al. 2014); and *fgf11*, member of the fibroblast growth factor (FGF) family, which is involved in development and morphogenesis (Tejedor et al. 2020). An enrichment analysis was conducted on the lists of genes located within these high-repeat-density regions for each species with g:Profiler. Genes associated with regulatory and developmental biological processes (e.g. "developmental process," "anatomical structure development," "animal organ development") were significantly overrepresented in the high-repeat-density regions for all species (Table S8; Fig. S5).

Genes Potentially Under Natural Selection and Divergence in Regulatory Regions

As an approach to identify potential genes under selection, we calculated the pairwise ratio between nonsynonymous and synonymous substitutions (dN/dS) for all genes between

Downloaded from https://academic.oup.com/gbe/article/17/11/evaf196/8303492 by guest on 27 January 2026

each species pair for the analyzed *Anolis* species (Table S9). We retained genes with dN/dS > 1 overlapping in at least two out of three comparisons for each species (Fig. S6). For *A. frenatus*, 16 genes overlapped including *mtpn*, a muscle growth factor that shows similar effects to *igf1* (Hayashi 2001; Mohammadabadi et al. 2021); and *pdzk1ip1*, which regulates and inhibits transforming growth factor (TGF-β) and bone morphogenic protein (BMP) signaling (Ikeno et al. 2019). For *A. auratus*, 12 genes overlapped, including *ramp2*, which regulates angiogenesis, cardiovascular development, and influences bone formation (Naot and Cornish 2008; Shindo et al. 2019); and *dcdc1*, associated with bone mineral density (Rivadeneira et al. 2009) and bone degradation in humans (Rossi et al. 2020). In *A. carolinensis*, we detected six overlapping genes, including *lep*, a gene relevant to lipid metabolism and energetic balance and that has thermogenic effects on skeletal muscle (Dulloo et al. 2002; Kaiyala et al. 2016; Fischer et al. 2020); *clps*, involved in lipid digestion (Brockman 2002); and *stard6*, associated with the intracellular transport of sterol and other lipids (Soccio et al. 2002). *A. sagrei* presented eight overlapping genes, including *ppdpf1*, associated with cell proliferation in multiple types of cancer (Zheng et al. 2022); and *s100a1*, which can regulate cell growth and proliferation (Zhang et al. 2021b). A gene enrichment analysis was run with g:Profiler for each species (Table S10). Among the over-represented GO terms, we detected "lipid catabolic process" and "digestion" for *A. carolinensis*, "positive regulation of developmental processes" for *A. auratus*, "regulation of muscle organ development" for *A. frenatus*, and "regulation of polarized epithelial cell differentiation" for *A. sagrei*.

To identify diverged regulatory regions, we identified genes with the top 1% of divergence in their putative promoter regions (1,000 bp upstream of the transcription start site, Andersson and Sandelin 2020) for each species pair (Table S11). We retained genes that overlapped in at least two out of three species comparisons. Within the overlapping genes identified for *A. frenatus*, we found *wnt4*, key ligand of Wnt/β-catenin signaling that controls development and cell differentiation (Zhang et al. 2021a); *traf4*, an important regulator of embryogenesis and bone development (Li et al. 2019); *hspg2*, which influences skeletal and cardiovascular development (Martinez et al. 2018); and *errfi1*, which affects cell growth by regulating epidermal growth factor receptor (EGFR) signaling (Cairns et al. 2018). In *A. carolinensis*, we detected genes associated with lipid metabolism like *plin3*, *lpin1*, and *ncoa1* (Csaki et al. 2013; Zhu et al. 2019; Wagner et al. 2021). For *A. auratus*, we found *cib2*, associated with mechanoelectrical transduction in auditory cells (Wang et al. 2017). In *A. sagrei*, we found *rab3d* involved in bone resorption (Zhu et al. 2016); and *optn*, a gene associated with autoimmune and neurodegenerative disorders (Mou et al. 2022).

We combined these genes with high divergence in the regulatory regions with the genes previously identified with dN/dS > 1 to generate our candidate gene set. We then used STRING v11 (Szklarczyk et al. 2019) to estimate gene interaction networks for genes in our combined candidate set to obtain an integrative view of evolutionary processes that spanned both regulatory and protein divergence (Fig. 4a). Some genes with dN/dS > 1 were embedded within gene interaction networks of genes with high divergence in regulatory regions (Figs. 4a and S7). For example, in *A. carolinensis*, several genes in the gene interaction network have functions associated with gene regulation, lipid metabolism, and mitochondria (Fig. 4a). The positively selected *lep* gene constitutes a central node in the gene interaction network and interacts with other elements of similar function that present high divergence in the regulatory regions.

Association With Phenotypic Traits

We characterized the realized climatic niche across the native distribution for the four *Anolis* species and detected that they have different climatic niches (Fig. S8). Among them, *A. carolinensis* occupies the coldest (Fig. 4b) and most thermally seasonal (Fig. 4c) environments. This is in accordance with genes with dN/dS > 1 and regulatory divergence mostly associated with biological functions that could influence cold tolerance such as lipid metabolism, mitochondrial function, and circulatory system (Fig. 4a).

The morphology of the four focal species was also analyzed (Fig. S9). *A. frenatus* is distinct in its larger body size (Fig. 5a). The genes *mtpn* and *pdzk1ip1* had dN/dS > 1 in *A. frenatus* with respect to the other three species and could influence its larger body size (Fig. 5c). In contrast, *A. auratus* is characterized by its unique tail elongation (Fig. 5b). We explored the morphology of the caudal vertebrae, and we found that the long tail in *A. auratus* is achieved by an elongation of the caudal vertebrae rather than an increase in the number of vertebrae when compared to the other species (Fig. 5d). The relative length of the trunk vertebrae of *A. auratus* did not differ from the other species (Fig. S10). *A. frenatus* also features a relatively longer tail and longer caudal vertebrae than *A. sagrei* and *A. carolinensis*, but not as long as *A. auratus* (Fig. 5d). Among the genes with dN/dS > 1 in *A. auratus*, we detected *ramp2* and *dcdc1*, which could be associated with the vertebral elongation phenotype (Fig. 5e).

Discussion

Genomic characteristics can influence speciation and promote phenotypic variation within adaptive radiations (Marques et al. 2019; Gillespie et al. 2020). Here, we explored the genomic variation, namely, chromosomal rearrangements and repeat element concentration, potentially contributing to diversity and phenotypic disparity within the *Anolis* radiation. Our results show examples of

Downloaded from https://academic.oup.com/gbe/article/17/11/evaf196/8303492 by guest on 27 January 2026

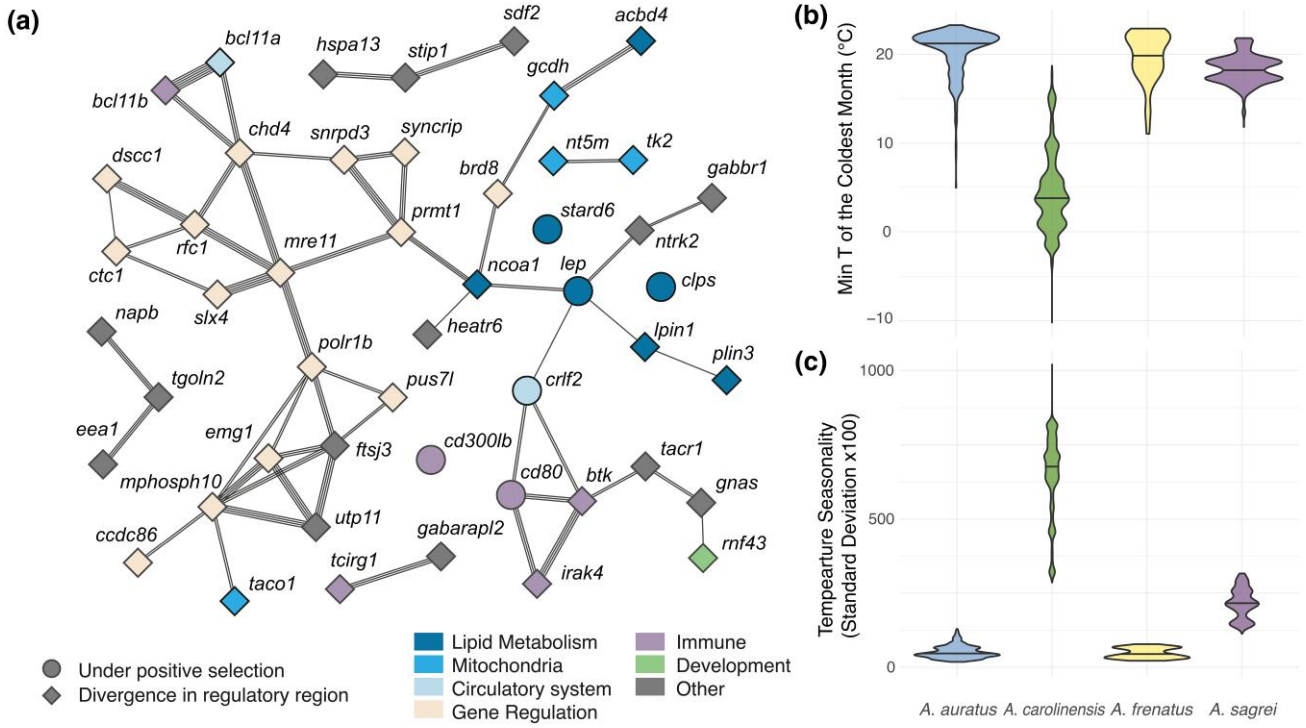

Fig. 4. Climatic niche characterization across the native distribution range of the four studied anole species. a) Gene interaction network for the genes with dN/dS > 1 and genes with high divergence on the promoter region for A. carolinensis. Line thickness represents the number of multiple evidence supporting the interaction between two genes. b) Minimum temperature of the coldest month. c) Temperature seasonality. A. carolinensis is the species inhabiting the coldest and more thermally seasonal environments.

major structural rearrangements, high densities of TEs around developmental genes, and potential signatures of natural selection and divergence on regulatory regions that enable the hypothesis formulation of the mechanisms that affect the unique phenotypes in these *Anolis* species.

Major Structural Rearrangements Within *Anolis*

Chromosome-level structural variations can directly influence speciation by disrupting meiosis in heterozygotes and reducing fertility in hybrids or generating barriers to gene flow (Olmo 2005; Lucek et al. 2023). Moreover, they can modify the gene regulation and recombination patterns (Mérot et al. 2020; Damas et al. 2021). Our synteny analysis detected major chromosomal rearrangements within *Anolis*. Chromosome fissions and fusions have been previously described as highly relevant in anoles (Castiglia et al. 2013; Gamble et al. 2014), but we also identified some translocations, inversions, and deletions among the analyzed species.

Chromosomes 1, 2, and 3 presented a substantial rearrangement in *A. frenatus* (Fig. 2b). Hi-C analysis suggests this is a true rearrangement and not a technical artifact given that contact maps show strong within-chromosome interactions and little to no interactions between these chromosomes (Figs. 2c and S2). In general, squamates show high synteny conservation for the major chromosomes (Koochekian et al. 2022; Davalos-Dehullu et al. 2023), and this result shows that at least one anole species deviates from the pattern. *A. frenatus* is part of the deeply divergent *Dactyloa* clade of *Anolis* (Fig. 1a; (Poe et al. 2017), and with our current sampling, we cannot determine if this mutation evolved uniquely in *A. frenatus* or is common to other species within *Dactyloa*. Chromosomes 1, 2, and 3 are bigger in other *Dactyloa* anoles when compared to non-*Dactyloa* karyotypes (Table S12), but a detailed genomic analysis including other species from the clade would be needed to determine the origin of this mutation. Nonetheless, the chromosomal breaks in *A. frenatus* were located in areas with a high density of genes with developmental functions (Fig. 2d), including some genes highly relevant to skeletal and muscle development and growth like *axin2*, *bmp2*, *ddit3*, and *twist2* (Dao et al. 2010; Shu et al. 2011; Liu et al. 2017; Zecchini et al. 2019). The major structural rearrangements could have altered the gene regulation patterns of these developmental genes adjacent to them (Mérot et al. 2020; Damas et al. 2021). This allows us to hypothesize that the structural rearrangements in *A. frenatus* (and potentially other *Dactyloa*) could have influenced the evolution of body size and morphology.

Downloaded from https://academic.oup.com/gbe/article/17/11/evaf196/8303492 by guest on 27 January 2026

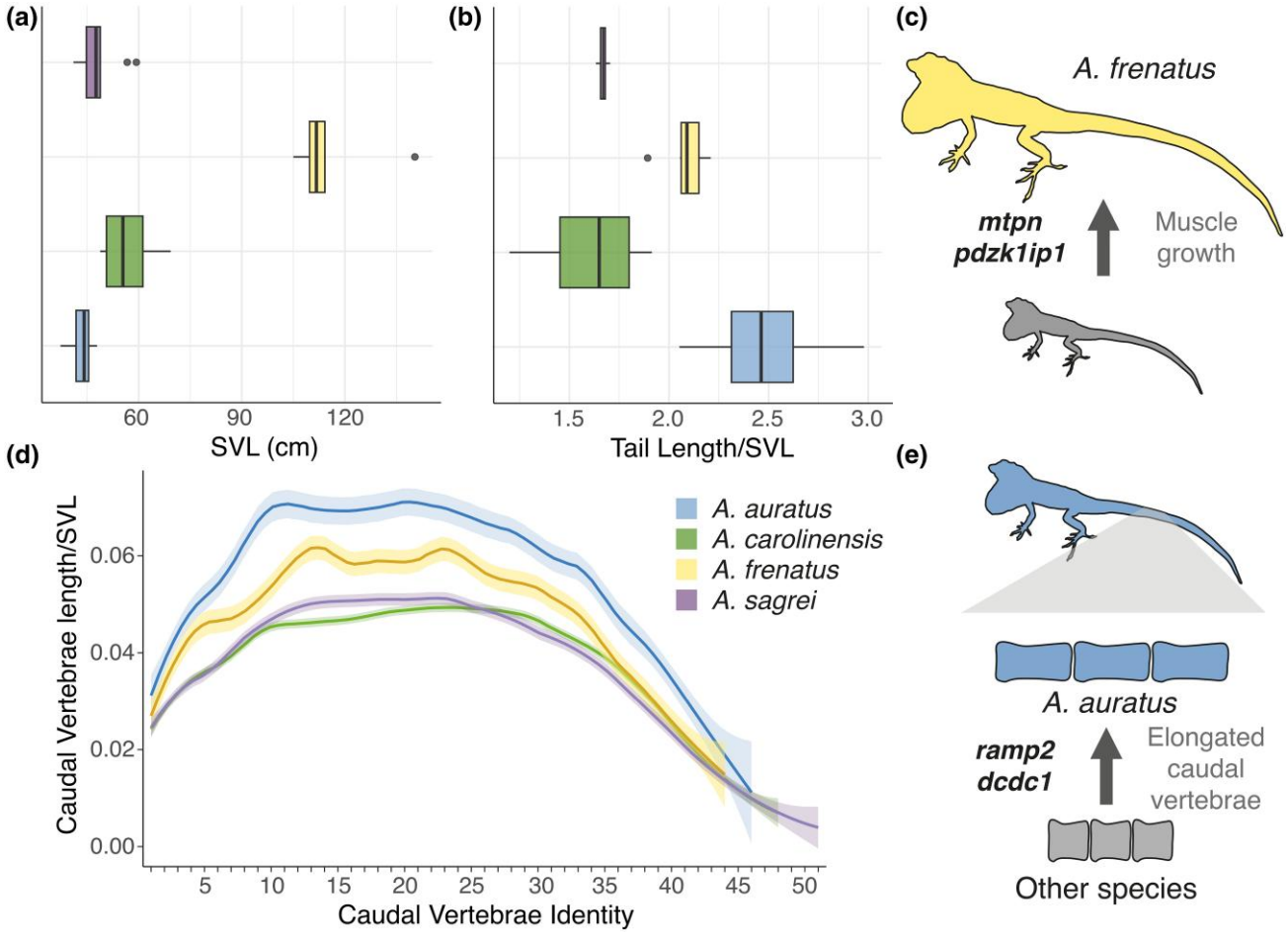

Fig. 5. Morphological variation in distinctive traits of the analyzed species. a) A. frenatus stands out for its large body size. b) A. auratus is characterized by a long tail. c) Selection on the mtpn and pdzk1ip1 genes could influence A. frenatus body size. d) The long tail in A. auratus is caused by an elongation of the caudal vertebrae rather than the addition of more vertebrae. e) Selection on ramp2 and dcdc1 could influence the vertebral elongation in A. auratus.

Our results also allowed us to explore patterns of sex chromosome evolution across *Anolis*. Anoles share a single ancestral XY sex chromosome system but have commonly experienced chromosomal fission and fusion, including fusions that involve sex chromosomes (Gamble et al. 2014; Rovatsos et al. 2014). In *A. sagrei*, the X chromosome (scaffold 7) has been reported as the fusion of chromosomes 9, 12, 13, and 18 from *A. carolinensis* (Kichigin et al. 2016; Giovannotti et al. 2017; Geneva et al. 2022). Further, Giovannotti et al. (2017) described chromosome 7 homology between *A. sagrei* and *Anolis valencienni*, both belonging to the *Norops* clade of anoles. Our results are consistent with this finding (Figs. 2a and S3) and expand the homology for the sex chromosome to all three analyzed *Norops* clade anoles (*A. auratus*, *A. apletophallus*, and *A. sagrei*), with only within-chromosome structural changes such as inversions and deletions differing among these species (Fig. S3). *Norops* is one of the most diverse clades within *Anolis* (Poe et al. 2017) with ~200 species. Our findings suggest that the X-autosome fusions detected in *A. sagrei* arose early in the clade (~40 Mya; Fig. 1) and highlight the relevance of sex chromosome evolution for anole diversification (Gamble et al. 2014; Rovatsos et al. 2014).

Key Developmental Genes in Repeat-Rich Regions in *Anolis* and Other Pleurodonts

Repeat elements can be a source of genetic variation because they can modify gene regulation patterns, be a source of mutations, and trigger structural rearrangements (Bourque et al. 2018; Schrader and Schmitz 2019). The genome-wide percentage of repeats was similar among species (Table 1), but *A. carolinensis* had a lower percentage of repeats, potentially due to the comparatively less complete and contiguous assembly currently available for this species (Alföldi et al. 2011). The relative composition of repeat families differed among genera, with anoles characterized by a higher abundance of DNA transposons and

Downloaded from https://academic.oup.com/gbe/article/17/11/evaf196/8303492 by guest on 27 January 2026

LINEs (Fig. S4) (as previously reported; Feiner 2019; Gable et al. 2023). Moreover, we found a high density of repeats associated with key developmental genes such as *notch4*, *fgf11*, and the *hoxB*, *hoxC*, and *hoxD* clusters in *Anolis* and the outgroups (Fig. 3; James et al. 2014; Mallo 2020; Tejedor et al. 2020). An enrichment analysis detected that genes located in repeat-rich regions were mostly associated with developmental and regulatory functions (Fig. S4, Table S6). For all analyzed species, the composition of repeat families within repeat-rich regions did not differ from their genome-wide relative abundance (Table S4). This suggests that the patterns of repeat accumulation are not biased toward a specific class of repeats. Other gene families, such as the major histocompatibility complex (MHC), have also been described to show a higher abundance of repeats in anoles versus other squamates (Card et al. 2022).

Feiner (2016, 2019) reported this unique pattern of repeat accumulation around the *hox* gene clusters in anoles, whereas other more distantly related squamates have a significantly lower number of repeats in these regions. Those studies, however, did not include other pleurodont lizards such as the phrynosomatids *U. nigricaudus* and *P. platyrhinos*. Thus, our analysis expands the pattern of repeat element accumulation to other genes that also affect development (Table S5) and indicates that this is not a feature exclusive to *Anolis* but is also present in other species from the Pleurodonta clade of Iguania. Pleurodont lizards include some of the most diverse vertebrate genera with respect to species number and morphological variation (e.g. *Anolis*, *Liolaemus*, *Sceloporus*; Blankers et al. 2013; Alencar et al. 2024). Therefore, the accumulation of repeat elements around developmental genes could be a source of genetic variation that fueled morphological innovation in pleurodont groups (Feiner 2019). Exploring the potential effects of the repeat accumulation on genetic and phenotypic variation for these lizard groups is key to understanding whether TE dynamics contribute to their evolvability and diversification. However, additional genomes assembled from within pleurodonts and other iguanians are needed to identify specifically when this pattern arose.

Potential Signatures of Selection on Coding Regions and Regulatory Divergence Could Influence Unique Phenotypes in *Anolis*

For the analyzed species, we detected some candidate genes potentially under selection and genes with high divergence in their regulatory regions that we can hypothesize to influence their unique phenotypes (Figs. 4 and S7). While phylogenetically explicit methods could provide better insight into the lineage-specific signatures of selection given the lack of evolutionary independence among our samples, we focused on pairwise comparisons because our heavily underrepresented sampling of the anole diversity (four out of over 400 species) could bias comparative analyses (Boettiger et al. 2012). Moreover, we acknowledge that our approach has more power to identify signatures of pervasive selection rather than episodic selection. Future work, combining more comprehensive sampling within *Anolis* with estimates of selection using a phylogenetic approach, has the potential to provide further powerful insights into the evolutionary dynamics of the genus.

A. carolinensis presented dN/dS > 1 and high regulatory divergence on genes potentially influencing cold adaptation. In general, ectotherm adaptation to cold environments involves physiological processes of oxygen consumption and blood circulation (Angilletta 2009; Campbell-Staton et al. 2018). Among the genes under selection in *A. carolinensis*, leptin (*lep*) was a central node in the gene interaction network (Fig. 4). Moreover, other genes associated with lipid metabolism (e.g. *clps*, *stard6*, *ncoa1*, *lpin1*, *plin3*) were also identified in our analysis. Lipid metabolism has been proposed as a potential thermal adaptation in ectotherms (Wollenberg Valero et al. 2014). For instance, it could be an alternative energy source during cold seasons with lower resource availability (Sun et al. 2022), or it could be associated with changes in cell membrane composition impacting fluidity in colder temperatures (Seebacher et al. 2009). Genes associated with lipid metabolism have been identified as undergoing accelerated evolution when comparing Cuban anole species with different thermal biology (Sakamoto et al. 2024). Furthermore, genes interacting with leptin and involved in lipid metabolism have been identified as being under-selection in *Anolis cybotes* populations inhabiting cold high-elevation environments (Rodríguez et al. 2017). Therefore, it is possible that changes in lipid metabolism could constitute an adaptation to cold environments in *A. carolinensis*. We also detected divergence in the regulatory region of genes associated with the circulatory system and mitochondria (Fig. 4). Populations of *A. carolinensis* inhabiting colder environments show lower oxygen consumption rates and signatures of selection and changes in the expression of genes associated with the circulatory system (Campbell-Staton et al. 2016, 2018). Thus, changes in these genes could enhance oxygen intake for low oxygen availability under cold temperatures in *A. carolinensis* versus other anole species.

A. auratus stands out for its long tail. This species is usually found on the grass in dense vegetation patches, and a long tail may provide better balance when walking or jumping across narrow perches (Gillis et al. 2009; Hsieh 2015). Body elongation is a convergent phenotype in several reptiles, and most species develop longer bodies through the addition of vertebrae (Bergmann and Morinaga 2019). However, the extremely long tail in *A. auratus* is achieved by elongation of the caudal vertebrae rather than the addition of more segments (Fig. 5d). The longest caudal

Downloaded from https://academic.oup.com/gbe/article/17/11/evaf196/8303492 by guest on 27 January 2026

vertebrae in *A. auratus* are located distal to the ninth caudal vertebrae (e.g. Ca10-21, Fig. 5d). In anoles, the *m. caudofemoralis longus* originates from the proximal caudal vertebrae (e.g. Ca2-8 in *A. sagrei*, Herrel et al. 2008; Ca2-9 in *Anolis heterodermus*, *Anolis tolimensis*, and *A. valencienni*, Herrel et al. 2008; Ríos-Orjuela et al. 2020; and Ca3-8 in *A. carolinensis*, Ritzman et al. 2012). This primary hip joint extensor is essential for locomotion and may also assist with lateral flexion of the tail when the hindlimb is fixed (Ritzman et al. 2012). Therefore, caudal vertebral elongation in *A. auratus* is most pronounced in a region of the tail that is less functionally constrained. The pattern of caudal vertebrae elongation in *A. auratus* is similar to that seen in the tail of arboreal *Peromyscus maniculatus* (Kingsley et al. 2024), the cervical vertebrae of giraffes (Agaba et al. 2016), the trunk of some plethodontid salamanders (Parra-Olea and Wake 2001), and some fish species (Ward and Mehta 2010). Among the mechanisms that could determine caudal vertebral elongation are genes associated with axial development and determinants of the caudal region such as the *hox13* genes, *fgf8*, or *fgfr1* (Agaba et al. 2016; Mallo 2018, 2020; Ye and Kimelman 2020; Kingsley et al. 2024). Nonetheless, genes positively selected in giraffes did not show dN/dS > 1 in *A. auratus* (Fig. S11). In our genetic data, we detected dN/dS > 1 in *ramp2* and *dcdc1*, which influence bone development (Naot and Cornish 2008; Rivadeneira et al. 2009). Heterozygote knockout mice for *ramp2* present skeletal abnormalities such as lower bone density and delayed development of the lumbar vertebrae, producing a similar pattern of vertebral elongation (Kadmiel et al. 2011). In *P. maniculatus*, *dcdc1* is located within a locus associated with TL (Kingsley et al. 2024). Thus, the mutations in these genes could contribute to the unique tail phenotype in *A. auratus*.

Finally, *A. frenatus* is characterized by a large body size and relatively long limbs. In general, vertebrate body size is determined by genes associated with insulin growth factors and growth hormone pathways (Kemper et al. 2012; Rotwein 2018; Beatty and Schwartz 2020; Silva et al. 2023). Our analysis identified some candidate genes potentially associated with large body size in *A. frenatus*. We detected dN/dS > 1 on the *mtpn* and *pdzk1ip1* genes, both involved in muscle development, growth, and morphogenesis (Hayashi 2001; Massagué 2012; Wang et al. 2014; Ikeno et al. 2019; Mohammadabadi et al. 2021). Injection of *mtpn* in mice produces increased body and muscle weights (Shiraishi et al. 2006). Moreover, among the genes that presented high divergence in regulatory regions for *A. frenatus*, we identified other genes highly relevant for development. For instance, *wnt4* can be modulated by the growth hormone (Vouyovitch et al. 2016), and mice with overexpression of *wnt4* present dwarfism (Lee and Behringer 2007). Further, knockout mice for *traf4* show reduced body weight compared with wild-type mice (Shiels et al. 2000). We interpret these results with caution because, given the phylogenetic distance between *A. frenatus* and the other study species, we cannot be certain whether these mutations are exclusive to *A. frenatus* or could be shared with other *Dactyloa* anoles.

Overall, the genes with dN/dS > 1 and with high divergence in their regulatory regions perform relevant biological functions that could affect the phenotypes of the analyzed species. This indicates that the combination of mechanisms acting at different hierarchical levels can aid in the generation of adaptive phenotypes in anoles. Changes in regulatory regions could provide more evolvability than changes in protein-coding sequences that are in general more constrained to mutations given their biological function (Hill et al. 2021; Sakamoto et al. 2024). Therefore, exploring the effects of regulatory sequence divergence and regulatory RNAs on gene expression and their impacts on species traits is key to understanding how this variation could promote anole phenotypic diversity.

Conclusions

Our analysis of novel genome assemblies of four anole species constitutes an early step to identifying the genomic variation that could contribute to the extensive phenotypic disparity among *Anolis* species. In *Anolis*, chromosome-level structural rearrangements could directly generate reproductive isolation and affect the gene regulation patterns of genes relevant to development and morphological configuration. Further, a high density of repeat elements close to key developmental genes could also contribute to variation in the expression of such genes. Finally, natural selection on few coding sequences but relevant to species traits, in addition to divergence in regulatory regions could also play a role in shaping phenotypic diversity. The interaction between these genomic characteristics and selection pressures potentially enabled the evolution of disparate phenotypes within anoles, but further analysis of a wider sample of high-quality genomes would help to formally address this hypothesis. We highlight that besides ecological opportunity, the genomic architecture of organisms can also influence adaptive radiations.

Methods

Sampling and Type Specimens

The *A. auratus* specimen was collected in Gamboa, Panama, and the *A. frenatus* specimen in Soberania National Park, Panama (Collecting Permits: SE/A-33-11 and SC/A-21-12, Autoridad Nacional de Ambiente, ANAM, Republic of Panama; IACUC Protocol: 2011-0616-2014-07 Smithsonian Tropical Research Institute). Additional samples of *A. carolinensis* and *A. sagrei* obtained from the Sullivan Company

Downloaded from https://academic.oup.com/gbe/article/17/11/evaf196/8303492 by guest on 27 January 2026

(Nashville, TN) and Marcus Cantos Reptiles (Fort Myers, FL) were included for morphological analyses (IACUC Protocol: Arizona State University 19-1053R and 12-1247R). Table S1 shows the number of individuals collected per species and locations used for reference genome assemblies and morphological analyses. Specimens were euthanized by intracoelomic injection of sodium pentobarbital (IACUC Protocols 09-1053R, 12-1274R, and 15-1416R ASU). The type specimens for the *A. auratus* and *A. frenatus* reference genomes corresponded to adult females.

Reference Genomes

We generated new reference genomes for *A. auratus* and *A. frenatus*. Skeletal muscle from the *A. auratus* type specimen and liver and heart from *A. frenatus* type specimen were sent for DNA extraction and whole-genome sequencing. The RUC_Aaur_2 and RUC_Afre_2 genomes were sequenced by Dovetail Genomics on an Illumina PE150 platform, de novo assembled with Meraculous v2.2.2.5 (Chapman et al. 2011). HiRise v2.1.6-072ca03871cc (Putnam et al. 2016) scaffolding was performed with Chicago and Hi-C chromatic conformation capture libraries. The published genome assemblies and annotations of *A. carolinensis* (AnoCar2.0, Alföldi et al. 2011; and Hi-C assembly from DNAzoo, Dudchenko et al. 2017, 2018) and *A. sagrei* (AnoSag2.1, Geneva et al. 2022) were included for comparative genomic analyses. Table 1 shows the assembly statistics for the four *Anolis* genomes. Additionally, we included the reference genome of the phrynosomatids *P. platyrhinos* (MUOH_PhPlat_1.1, Koochekian et al. 2022) and *U. nigricaudus* (ASU_Uro_nig_1, Davalos-Dehullu et al. 2023) for some comparative genomic analyses.

A genome annotation was generated for *A. auratus* and *A. frenatus*. For each species, repeats were identified on the genome sequences by using RepeatModeler v2.0.1 (Flynn et al. 2020), and then repeat elements were soft-masked on the assembly with RepeatMasker v4.1.1 (Smit et al. 2015). To aid in annotation, we generated a de novo transcriptome for each species using tail and ovary/yolk for *A. auratus* and brain and ovary for *A. frenatus*. Tissue samples were collected from the same animals used for genome sequencing. Tissues were sent to the Yale Center for Genomic Analyses (YCGA; West Haven, CT) for RNA extraction, cDNA poly-A-enriched Illumina library preparation, and sequencing on an Illumina NovaSeq S4 platform using 150-bp paired-end reads. Read quality was assessed with FastQC v0.11.7 (Andrews 2010), and reads were trimmed with TrimGalore v0.6.8 (Krueger 2015). Then a de novo transcriptome assembly was generated with Trinity v2.12.0 (Grabherr et al. 2011). The generated transcriptomes were used as evidence for each species genome annotation.

Multiple iterations of Maker v3.01.03 (Campbell et al. 2014) were run to annotate the genomes. We used the species-specific transcripts, and the protein-coding sequences from *A. carolinensis* and *A. sagrei* as evidence. A first round of Maker was run for aligning and mapping transcript and protein evidence. Then, two additional rounds of ab initio gene model prediction using Augustus v3.4.0 (Stanke et al. 2006) and SNAP v2006-07-28 (Korf 2004) were run. After each round of Maker, the Annotation Edit Distance (AED) was recorded, and annotation completeness was assessed with BUSCO v5.4.2 (Simão et al. 2015) on the predicted transcripts obtained from Maker, comparing against the eukaryote and sauropsid gene datasets.

Chromosome-Level Structural Rearrangements

We investigated synteny among the main scaffolds from the four analyzed *Anolis* species along with the phrynosomatids *P. platyrhinos* and *U. nigricaudus* by in silico chromosome painting. For this analysis, we used the high-contiguity DNAzoo Hi-C-scaffolded genome assembly of *A. carolinensis* (Dudchenko et al. 2017, 2018). All species were compared against the *A. sagrei* genome as a reference because it is the species with the most contiguous and complete genome among our samples (Geneva et al. 2022). The first 14 scaffolds from *A. sagrei*, representative of its chromosomes, were split in chunks of 100 bp with "faSplit" v438 from the UCSC Bioinformatic Utilities (Kuhn et al. 2013). Then, we used blastn v2.10.0 (Camacho et al. 2009) to map each fragment onto five other species' genome. We retained matches with at least 50-bp length and that were contiguous in at least five matches (Koochekian et al. 2022). To further explore the chromosome X evolution within *Anolis*, we compared chromosome 7 from *A. sagrei* to the closely related *A. apletophallus* (Pirani et al. 2023) following the same methodology.

Hi-C Data Analysis

Link density histograms were generated with Juicer v2.0 (Durand et al. 2016) by mapping paired reads from the Hi-C libraries for *A. auratus* and *A. frenatus* to the finished genome assembly to assess chromatin conformation and to validate our chromosomal rearrangements. Hi-C contact maps were visualized with Juicebox v1.9.8 (Dudchenko et al. 2018).

Developmental Genes Located in *A. frenatus* Scaffolds 1, 2, and 3 Rearrangement

We explored which genes were located adjected to the rearrangement among scaffolds 1, 2, and 3 detected between *A. frenatus* and *A. sagrei*. For this, we pulled from the *A. sagrei* annotation the genes located within 1 Mb from the scaffold breakpoints identified with the synteny analysis. We performed an enrichment analysis on the

Downloaded from https://academic.oup.com/gbe/article/17/11/evaf196/8303492 by guest on 27 January 2026

genes located in these regions with g:Profiler ve111_eg58_p18_30541362 (Kolberg et al. 2023) to assess which biological processes were overrepresented in that gene list. Then, we extracted the list of genes present in scaffolds 1, 2, and 3 in *A. frenatus* to identify if the chromosomal breaks were located in hotspots of genes with developmental function. We identified and extracted all the GO terms included in the list of genes located on each scaffold with g:Profiler using *Homo sapiens* as a reference, and we retained only the genes matching GO terms that included any of the following keywords: "development," "morpho," "growth," or "organ." We then calculated the number of genes with those developmental functions along each chromosome in 500-kb windows in R v4.1.2 (R Core Team 2022) with a custom script.

Repeat Density Through the Genomes

For *A. auratus*, *A. frenatus*, *A. sagrei*, *U. nigricaudus*, and *P. platyrhinos*, we calculated the repeat density for each one of the six largest scaffolds. First, we reclassified repeat families for the annotations of *U. nigricaudus*, *P. platyrhinos*, and *A. sagrei*, following the same methodology used for *A. auratus* and *A. frenatus*. We compared the repeat family composition for the six largest scaffolds among the five species with Fisher's exact test in R. Then, the number of repeats was calculated in 500-kb windows, and we retained repeats longer than 50 bp and with a score value over 10 (Feiner 2016). Then, we selected the 500-kb windows corresponding to the highest 5% of repeat density per scaffold for each species with a custom script in R. To assess if those regions were enriched in a particular class of repeats, we compared the repeat family composition of the repeat-rich regions against the six largest scaffolds for each species with Fisher's exact test. Then, we identified the genes located within those high-repeat-density regions using the respective genome annotations. An enrichment analysis was performed to identify the most represented GO categories on the list of genes situated in high-repeat regions for each species with g:Profiler, and the enriched GO terms were semantically organized and visualized with Revigo v1.8.1 (Supek et al. 2011).

Identification of Genes Potentially Under Positive Selection and Regulatory Elements With High Divergence

We looked for genes potentially under positive selection among the four *Anolis* species by calculating the ratio between nonsynonymous and synonymous mutations (dN/dS) between orthologs from species pairs with the "orthologr" package (Drost et al. 2015) in R using Comeron's (1995) method. To identify genes with dN/dS > 1 in each species, we retained the genes overlapping in at least two out of three comparisons between the focal and the other three species. We focused on pairwise comparisons instead of phylogenetically explicit methods to detect genes under selection, because heavily underrepresented phylogenies could bias comparative analyses (Boettiger et al. 2012). Moreover, having fewer than 10 species significantly decreases the statistical power when using phylogeny-based approaches (Murrell et al. 2012). An enrichment analysis was performed on the list of positively selected genes with g:Profiler to identify the most represented GO terms for each species, using *H. sapiens* as a reference.

To assess regulatory regions with high divergence, we focused on 1,000 kb upstream of the transcription start, which includes the promoter region (Andersson and Sandelin 2020). We compared orthologs between species pairs previously identified with "orthologr" in R. Each ortholog pair was aligned with MAFFT v7.520 (Katoh and Standley 2013), and the genetic distance between aligned orthologs was estimated with the "bio3d" package (Grant et al. 2006) in R. We considered the genes with the top 1% of genetic distance as genes with the highest divergence in their regulatory regions between species pairs. For each species, we retained the genes overlapping in at least two out of three comparisons. Finally, we used STRING v12.0 (Szklarczyk et al. 2019) to evaluate gene interactions among the genes under selection and the genes with high regulatory divergence for each species.

Climatic Niche Analyses

For each species, occurrence records were obtained from the Global Biodiversity Information Facility (GBIF.2021). Occurrences were deduplicated and manually curated to accurately represent the native distribution of each species. The final dataset included 881 occurrences for *A. auratus*, 175 for *A. frenatus*, 27,546 for *A. carolinensis*, and 24,419 for *A. sagrei*. Raster data for 19 bioclimatic variables with 1 km^2 of spatial resolution were obtained from the WorldClim v2 database (Fick and Hijmans 2017). For each occurrence point, the corresponding values of the 19 bioclimatic variables were obtained using QGIS v3.16.16-Hannover (QGIS.org 2020). We qualitatively compared the climatic niche among the four analyzed species. Climatic variation was visualized with a principal component analysis (PCA) in R, and the main variables differentiating species were identified based on their loadings in the first two principal components.

Morphological Analyses

Additional samples for the four *Anolis* species were included for morphological analyses. Skeletal data were obtained from osteological preparations following Tollis et al.'s (2018) modification of amphibian protocols or from micro-computed tomography (micro-CT) images collected in a Siemens Inveon micro-CT scanner at the RII

Downloaded from https://academic.oup.com/gbe/article/17/11/evaf196/8303492 by guest on 27 January 2026

Translational Bioimaging Resource at the University of Arizona (Table S2). For skeletal preparations, individuals were photographed with a scale in a stereodissecting microscope (Nikon SMZ800 with Coolpix 995 digital camera), and morphological traits were measured with ImageJ v1.53k (Schneider et al. 2012). For micro-CT scans, digital images were analyzed and measured with InVesalius v3.1.1 (Amorim et al. 2015). For each species, we measured snout–vent length (SVL), axilla–groin distance (AGD), forelimb total length (FLL), forelimb autopod length, forelimb stylopod length, forelimb zeugopod length, hindlimb total length (HLL), hindlimb autopod length, hindlimb stylopod length, hindlimb zeugopod length, head width (HW), head length (HL), head height (HH), and TL. We also analyzed the osteology of the caudal vertebrae for the four *Anolis* species. For this, we measured the distance from the distal end of the cotyle to the proximal tip of the condyle on each caudal vertebra. All measurements apart from SVL were standardized by dividing by the distance from the snout to the end of the sacral vertebrae as an approximation to body size. We compared micro-CT and skeletal preparation measurements with a paired *T*-test to assess possible bias in the sampling methodology (Table S13).

Funding

This project was supported by funding from National Science Foundation grants DEB-1927194 to AJG and JL, and DGE-2152059 to AJG, and the College of Liberal Arts and Sciences at Arizona State University (ASU) to KK. RAD was supported by the Doctoral scholarship 72200094 (ANID, Chile) and the Peabody Family Memorial Scholarship. Support for EL was provided by the ASU School of Life Sciences Undergraduate Research Program.

Data Availability

All raw read files have been accessioned to the NCBI SRA under BioProject #PRJNA1096315. Final genome assemblies and annotations have been accessioned to the Harvard Dataverse (https://doi.org/10.7910/DVN/F9NDWL).

Supplementary Material

Supplementary material is available at *Genome Biology and Evolution* online.

Literature Cited

Agaba M, et al. Giraffe genome sequence reveals clues to its unique morphology and physiology. Nat Commun. 2016:7:11519. https://doi.org/10.1038/ncomms11519.

Alencar LRV, et al. Opportunity begets opportunity to drive macroevolutionary dynamics of a diverse lizard radiation. Evol Lett. 2024:8:623–637. https://doi.org/10.1093/evlett/qrae022.

Alföldi J, et al. The genome of the green anole lizard and a comparative analysis with birds and mammals. Nature. 2011:477:587–591. https://doi.org/10.1038/nature10390.

Amorim P, et al. InVesalius: an interactive rendering framework for health care support. In: Bebis G, Boyle R, Parvin B, Koracin D, Pavlidis I, editors. Advances in visual computing. Springer International Publishing; 2015. p. 45–54. Lecture Notes in Computer Science Vol. 9474.

Andersson R, Sandelin A. Determinants of enhancer and promoter activities of regulatory elements. Nat Rev Genet. 2020:21:71–87. https://doi.org/10.1038/s41576-019-0173-8.

Andrews S. FastQC: a quality control tool for high throughput sequence data. 2010. https://www.bioinformatics.babraham.ac.uk/projects/fastqc/. Accessed 2022 August 10.

Angilletta MJ Jr. Thermal Adaptation. Oxford University Press; 2009.

Beatty AE, Schwartz TS. Gene expression of the IGF hormones and IGF binding proteins across time and tissues in a model reptile. Physiol Genomics. 2020:52:423–434. https://doi.org/10.1152/physiolgenomics.00059.2020.

Bergmann PJ, Morinaga G. The convergent evolution of snake-like forms by divergent evolutionary pathways in squamate reptiles. Evolution. 2019:73:481–496. https://doi.org/10.1111/evo.13651.

Blankers T, Townsend TM, Pepe K, Reeder TW, Wiens JJ. Contrasting global-scale evolutionary radiations: phylogeny, diversification, and morphological evolution in the major clades of iguanian lizards: global radiations in lizards. Biol J Linn Soc Lond. 2013:108:127–143. https://doi.org/10.1111/j.1095-8312.2012.01988.x.

Boettiger C, Coop G, Ralph P. Is your phylogeny informative? Measuring the power of comparative methods. Evolution. 2012:66:2240–2251. https://doi.org/10.1111/j.1558-5646.2011.01574.x.

Bourque G, et al. Ten things you should know about transposable elements. Genome Biol. 2018:19:199. https://doi.org/10.1186/s13059-018-1577-z.

Brawand D, et al. The genomic substrate for adaptive radiation in African cichlid fish. Nature. 2014:513:375–381. https://doi.org/10.1038/nature13726.

Brockman H. Colipase-induced reorganization of interfaces as a regulator of lipolysis. Colloids Surf B Biointerfaces. 2002:26:102–111. https://doi.org/10.1016/s0927-7765(02)00031-0.

Butler MA, Sawyer SA, Losos JB. Sexual dimorphism and adaptive radiation in *Anolis* lizards. Nature. 2007:447:202–205. https://doi.org/10.1038/nature05774.

Cairns J, et al. Differential roles of ERRFI1 in EGFR and AKT pathway regulation affect cancer proliferation. EMBO Rep. 2018:19:e44767. https://doi.org/10.15252/embr.201744767.

Camacho C, et al. BLAST+: architecture and applications. BMC Bioinformatics. 2009:10:421. https://doi.org/10.1186/1471-2105-10-421.

Campbell MS, Holt C, Moore B, Yandell M. Genome annotation and curation using MAKER and MAKER-P. Curr Protoc Bioinformatics. 2014:48:4.11.1–4.11.39. https://doi.org/10.1002/0471250953.bi0411s48.

Campbell-Staton SC, Bare A, Losos JB, Edwards SV, Cheviron ZA. Physiological and regulatory underpinnings of geographic variation in reptilian cold tolerance across a latitudinal cline. Mol Ecol. 2018:27:2243–2255. https://doi.org/10.1111/mec.14580.

Campbell-Staton SC, Edwards SV, Losos JB. Climate-mediated adaptation after mainland colonization of an ancestrally subtropical island lizard, *Anolis carolinensis*. J Evol Biol. 2016:29:2168–2180. https://doi.org/10.1111/jeb.12935.

Card DC, et al. Structure and evolution of the squamate major histocompatibility complex as revealed by two *Anolis* lizard genomes. Front Genet. 2022:13:979746. https://doi.org/10.3389/fgene.2022.979746.

Downloaded from https://academic.oup.com/gbe/article/17/11/evaf196/8303492 by guest on 27 January 2026

Castiglia R, Flores-Villela O, Bezerra AMR, Muñoz A, Gornung E. Pattern of chromosomal changes in 'beta' *Anolis* (*Norops* group) (Squamata: Polychrotidae) depicted by an ancestral state analysis. Zool Stud. 2013:52:60. https://doi.org/10.1186/1810-522x-52-60.

Chapman JA, et al. Meraculous: de novo genome assembly with short paired-end reads. PLoS One. 2011:6:e23501. https://doi.org/10.1371/journal.pone.0023501.

Comeron JM. A method for estimating the numbers of synonymous and nonsynonymous substitutions per site. J Mol Evol. 1995:41:1152–1159. https://doi.org/10.1007/bf00173196.

Csaki LS, et al. Lipins, lipinopathies, and the modulation of cellular lipid storage and signaling. Prog Lipid Res. 2013:52:305–316. https://doi.org/10.1016/j.plipres.2013.04.001.

Damas J, Corbo M, Lewin HA. Vertebrate chromosome evolution. Annu Rev Anim Biosci. 2021:9:1–27. https://doi.org/10.1146/annurev-animal-020518-114924.

Dao DY, et al. Axin2 regulates chondrocyte maturation and axial skeletal development. J Orthop Res. 2010:28:89–95. https://doi.org/10.1002/jor.20954.

Davalos-Dehullu E, et al. Chromosome-level genome assembly of the blacktail brush lizard, *Urosaurus nigricaudus*, reveals dosage compensation in an endemic lizard. Genome Biol Evol. 2023:15:evad210. https://doi.org/10.1093/gbe/evad210.

Di-Poï N, et al. Changes in Hox genes' structure and function during the evolution of the squamate body plan. Nature. 2010:464:99–103. https://doi.org/10.1038/nature08789.

Drost H-G, Gabel A, Grosse I, Quint M. Evidence for active maintenance of phylotranscriptomic hourglass patterns in animal and plant embryogenesis. Mol Biol Evol. 2015:32:1221–1231. https://doi.org/10.1093/molbev/msv012.

Dudchenko O, et al. The Juicebox Assembly Tools module facilitates de novo assembly of mammalian genomes with chromosome-length scaffolds for under $1000. bioRxiv 254797. https://doi.org/10.1101/254797, 28 January 2018, preprint: not peer reviewed.

Dudchenko O, et al. De novo assembly of the *Aedes aegypti* genome using Hi-C yields chromosome-length scaffolds. Science. 2017:356:92–95. https://doi.org/10.1126/science.aal3327.

Dulloo AG, et al. Leptin directly stimulates thermogenesis in skeletal muscle. FEBS Lett. 2002:515:109–113. https://doi.org/10.1016/s0014-5793(02)02449-3.

Duncan CA, Cohick WS, John-Alder HB. Testosterone reduces growth and hepatic *IGF-1* mRNA in a female-larger lizard, *Sceloporus undulatus*: evidence of an evolutionary reversal in growth regulation. Integr Org Biol. 2020:2:obaa036. https://doi.org/10.1093/iob/obaa036.

Durand NC, et al. Juicer provides a one-click system for analyzing loop-resolution Hi-C experiments. Cell Syst. 2016:3:95–98. https://doi.org/10.1016/j.cels.2016.07.002.

Edelman NB, et al. Genomic architecture and introgression shape a butterfly radiation. Science. 2019:366:594–599. https://doi.org/10.1126/science.aaw2090.

Farleigh K, et al. Signals of differential introgression in the genome of natural hybrids of Caribbean anoles. Mol Ecol. 2023:32:6000–6017. https://doi.org/10.1111/mec.17170.

Feiner N. Accumulation of transposable elements in *Hox* gene clusters during adaptive radiation of *Anolis* lizards. Proc R Soc Lond B Biol Sci. 2016:283:20161555. https://doi.org/10.1098/rspb.2016.1555.

Feiner N. Evolutionary lability in *Hox* cluster structure and gene expression in *Anolis* lizards. Evol Lett. 2019:3:474–484. https://doi.org/10.1002/evl3.131.

Fick SE, Hijmans RJ. WorldClim 2: new 1-km spatial resolution climate surfaces for global land areas. Int J Climatol. 2017:37:4302–4315. https://doi.org/10.1002/joc.5086.

Fischer AW, Cannon B, Nedergaard J. Leptin: is it thermogenic? Endocr Rev. 2020:41:232–260. https://doi.org/10.1210/endrev/bnz016.

Flynn JM, et al. RepeatModeler2 for automated genomic discovery of transposable element families. Proc Natl Acad Sci U S A. 2020:117:9451–9457. https://doi.org/10.1073/pnas.1921046117.

Gable SM, et al. The state of squamate genomics: past, present, and future of genome research in the most speciose terrestrial vertebrate order. Genes (Basel). 2023:14:1387. https://doi.org/10.3390/genes14071387.

Gamble T, Geneva AJ, Glor RE, Zarkower D. *Anolis* sex chromosomes are derived from a single ancestral pair. Evolution. 2014:68:1027–1041. https://doi.org/10.1111/evo.12328.

GBIF.Org. Occurrence Download. 29298189. 2021. https://doi.org/10.15468/dl.tqhdns.

Geneva AJ, et al. Chromosome-scale genome assembly of the brown anole (*Anolis sagrei*), an emerging model species. Commun Biol. 2022:5:1126. https://doi.org/10.1038/s42003-022-04074-5.

Gillespie RG, et al. Comparing adaptive radiations across space, time, and taxa. J Hered. 2020:111:1–20. https://doi.org/10.1093/jhered/esz064.

Gillis GB, Bonvini LA, Irschick DJ. Losing stability: tail loss and jumping in the arboreal lizard *Anolis carolinensis*. J Exp Biol. 2009:212:604–609. https://doi.org/10.1242/jeb.024349.

Giovannotti M, et al. New insights into sex chromosome evolution in anole lizards (Reptilia, Dactyloidae). Chromosoma. 2017:126:245–260. https://doi.org/10.1007/s00412-016-0585-6.

Grabherr MG, et al. Full-length transcriptome assembly from RNA-Seq data without a reference genome. Nat Biotechnol. 2011:29:644–652. https://doi.org/10.1038/nbt.1883.

Grant BJ, Rodrigues APC, ElSawy KM, McCammon JA, Caves LSD. Bio3d: an R package for the comparative analysis of protein structures. Bioinformatics. 2006:22:2695–2696. https://doi.org/10.1093/bioinformatics/btl461.

Gunderson AR, Mahler DL, Leal M. Thermal niche evolution across replicated *Anolis* lizard adaptive radiations. Proc Biol Sci. 2018:285:20172241. https://doi.org/10.1098/rspb.2017.2241.

Han F, et al. Gene flow, ancient polymorphism, and ecological adaptation shape the genomic landscape of divergence among Darwin's finches. Genome Res. 2017:27:1004–1015. https://doi.org/10.1101/gr.212522.116.

Hayashi T. S-myotrophin promotes the hypertrophy of myotube as insulin-like growth factor-I does. Int J Biochem Cell Biol. 2001:33:831–838. https://doi.org/10.1016/s1357-2725(01)00035-8.

Herrel A, Vanhooydonck B, Porck J, Irschick DJ. Anatomical basis of differences in locomotor behavior in *Anolis* lizards: a comparison between two ecomorphs. Bull Mus Comp Zool. 2008:159:213–238. https://doi.org/10.3099/0027-4100-159.4.213.

Hill MS, Vande Zande P, Wittkopp PJ. Molecular and evolutionary processes generating variation in gene expression. Nat Rev Genet. 2021:22:203–215. https://doi.org/10.1038/s41576-020-00304-w.

Hsieh ST. Tail loss and narrow surfaces decrease locomotor stability in the arboreal green anole lizard (*Anolis carolinensis*). J Exp Biol. 2015:219:364–373. https://doi.org/10.1242/jeb.124958.

Huie JM, Prates I, Bell RC, De Queiroz K. Convergent patterns of adaptive radiation between island and mainland *Anolis* lizards. Biol J Linn Soc Lond. 2021:134:85–110. https://doi.org/10.1093/biolinnean/blab072.

Ikeno S, et al. PDZK1-interacting protein 1 (PDZK1IP1) traps Smad4 protein and suppresses transforming growth factor-β (TGF-β) signaling. J Biol Chem. 2019:294:4966–4980. https://doi.org/10.1074/jbc.ra118.004153.

James AC, et al. Notch4 reveals a novel mechanism regulating Notch signal transduction. Biochim Biophys Acta. 2014:1843:1272–1284. https://doi.org/10.1016/j.bbamcr.2014.03.015.

Downloaded from https://academic.oup.com/gbe/article/17/11/evaf196/8303492 by guest on 27 January 2026

Kadmiel M, et al. Research resource: haploinsufficiency of receptor activity-modifying protein-2 (Ramp2) causes reduced fertility, hyperprolactinemia, skeletal abnormalities, and endocrine dysfunction in mice. Mol Endocrinol. 2011:25:1244–1253. https://doi.org/10.1210/me.2010-0400.

Kaiyala KJ, Ogimoto K, Nelson JT, Muta K, Morton GJ. Physiological role for leptin in the control of thermal conductance. Mol Metab. 2016:5:892–902. https://doi.org/10.1016/j.molmet.2016.07.005.

Kanamori S, et al. Draft genome of six Cuban *Anolis* lizards and insights into genetic changes during their diversification. BMC Ecol Evo. 2022:22:129. https://doi.org/10.1186/s12862-022-02086-7.

Katoh K, Standley DM. MAFFT multiple sequence alignment software version 7: improvements in performance and usability. Mol Biol Evol. 2013:30:772–780. https://doi.org/10.1093/molbev/mst010.

Kemper KE, Visscher PM, Goddard ME. Genetic architecture of body size in mammals. Genome Biol. 2012:13:244. https://doi.org/10.1186/gb-2012-13-4-244.

Kichigin IG, et al. Evolutionary dynamics of *Anolis* sex chromosomes revealed by sequencing of flow sorting-derived microchromosome-specific DNA. Mol Genet Genomics. 2016:291:1955–1966. https://doi.org/10.1007/s00438-016-1230-z.

Kingsley EP, et al. Adaptive tail-length evolution in deer mice is associated with differential Hoxd13 expression in early development. Nat Ecol Evol. 2024:8:791–805. https://doi.org/10.1038/s41559-024-02346-3.

Kolberg L, et al. G:profiler—interoperable web service for functional enrichment analysis and gene identifier mapping (2023 update). Nucleic Acids Res. 2023:51:W207–W212. https://doi.org/10.1093/nar/gkad347.

Koochekian N, et al. A chromosome-level genome assembly and annotation of the desert horned lizard, *Phrynosoma platyrhinos*, provides insight into chromosomal rearrangements among reptiles. GigaScience. 2022:11:giab098. https://doi.org/10.1093/gigascience/giab098.

Korf I. Gene finding in novel genomes. BMC Bioinformatics. 2004:5:59. https://doi.org/10.1186/1471-2105-5-59.

Kozak KM, Joron M, McMillan WO, Jiggins CD. Rampant genome-wide admixture across the *Heliconius* radiation. Genome Biol Evol. 2021:13:evab099. https://doi.org/10.1093/gbe/evab099.

Krueger F. TrimGalore!: a wrapper around Cutadapt and FastQC to consistently apply adapter and quality trimming to FastQ files, with extra functionality for RRBS data. 2015. https://github.com/FelixKrueger/TrimGalore. Accessed 2022 August 10.

Kuhn RM, Haussler D, Kent WJ. The UCSC genome browser and associated tools. Brief Bioinform. 2013:14:144–161. https://doi.org/10.1093/bib/bbs038.

Lee H-H, Behringer RR. Conditional expression of Wnt4 during chondrogenesis leads to dwarfism in mice. PLoS One. 2007:2:e450. https://doi.org/10.1371/journal.pone.0000450.

Lewis JJ, Reed RD. Genome-wide regulatory adaptation shapes population-level genomic landscapes in *Heliconius*. Mol Biol Evol. 2019:36:159–173. https://doi.org/10.1093/molbev/msy209.

Li J, et al. TRAF4 positively regulates the osteogenic differentiation of mesenchymal stem cells by acting as an E3 ubiquitin ligase to degrade Smurf2. Cell Death Differ. 2019:26:2652–2666. https://doi.org/10.1038/s41418-019-0328-3.

Liu N, et al. A Twist2-dependent progenitor cell contributes to adult skeletal muscle. Nat Cell Biol. 2017:19:202–213. https://doi.org/10.1038/ncb3477.

Losos JB. Ecomorphology, performance capability, and scaling of west Indian *Anolis* lizards: an evolutionary analysis. Ecol Monogr. 1990:60:369–388. https://doi.org/10.2307/1943062.

Losos JB. Lizards in an evolutionary tree: ecology and adaptive radiation of anoles. University of California Press; 2011.

Losos JB, Andrews RM, Sexton OJ, Schuler AL. Behavior, ecology, and locomotor performance of the giant anole, *Anolis frenatus*. Caribb J Sci. 1991:27:173–179.

Lucek K, et al. The impact of chromosomal rearrangements in speciation: from micro- to macroevolution. Cold Spring Harb Perspect Biol. 2023:15:a041447. https://doi.org/10.1101/cshperspect.a041447.

Mahler DL, Revell LJ, Glor RE, Losos JB. Ecological opportunity and the rate of morphological evolution in the diversification of greater Antillean anoles: opportunity and rate in *Anolis* lizards. Evolution. 2010:64:2731–2745. https://doi.org/10.1111/j.1558-5646.2010.01026.x.

Mallo M. Reassessing the role of Hox genes during vertebrate development and evolution. Trends Genet. 2018:34:209–217. https://doi.org/10.1016/j.tig.2017.11.007.

Mallo M. The vertebrate tail: a gene playground for evolution. Cell Mol Life Sci. 2020:77:1021–1030. https://doi.org/10.1007/s00018-019-03311-1.

Marques DA, Meier JI, Seehausen O. A combinatorial view on speciation and adaptive radiation. Trends Ecol Evol. 2019:34:531–544. https://doi.org/10.1016/j.tree.2019.02.008.

Martin CH, Richards EJ. The paradox behind the pattern of rapid adaptive radiation: how can the speciation process sustain itself through an early burst? Annu Rev Ecol Evol Syst. 2019:50:569–593. https://doi.org/10.1146/annurev-ecolsys-110617-062443.

Martinez JR, Dhawan A, Farach-Carson MC. Modular proteoglycan perlecan/HSPG2: mutations, phenotypes, and functions. Genes (Basel). 2018:9:556. https://doi.org/10.3390/genes9110556.

Massagué J. TGFβ signalling in context. Nat Rev Mol Cell Biol. 2012:13:616–630. https://doi.org/10.1038/nrm3434.

McGee MD, et al. The ecological and genomic basis of explosive adaptive radiation. Nature. 2020:586:75–79. https://doi.org/10.1038/s41586-020-2652-7.

Mérot C, Oomen RA, Tigano A, Wellenreuther M. A roadmap for understanding the evolutionary significance of structural genomic variation. Trends Ecol Evol. 2020:35:561–572. https://doi.org/10.1016/j.tree.2020.03.002.

Mohammadabadi M, Bordbar F, Jensen J, Du M, Guo W. Key genes regulating skeletal muscle development and growth in farm animals. Animals (Basel). 2021:11:835. https://doi.org/10.3390/ani11030835.

Mou Y, et al. OPTN variants in ALS cases: a case report of a novel mutation and literature review. Neurol Sci. 2022:43:5391–5396. https://doi.org/10.1007/s10072-022-06125-5.

Muñoz MM, Frishkoff LO, Pruett J, Mahler DL. Evolution of a model system: new insights from the study of *Anolis* lizards. Annu Rev Ecol Evol Syst. 2023:54:475–503. https://doi.org/10.1146/annurev-ecolsys-110421-103306.

Murrell B, et al. Detecting individual sites subject to episodic diversifying selection. PLoS Genet. 2012:8:e1002764. https://doi.org/10.1371/journal.pgen.1002764.

Naot D, Cornish J. The role of peptides and receptors of the calcitonin family in the regulation of bone metabolism. Bone. 2008:43:813–818. https://doi.org/10.1016/j.bone.2008.07.003.

Olmo E. Rate of chromosome changes and speciation in reptiles. Genetica. 2005:125:185–203. https://doi.org/10.1007/s10709-005-8008-2.

Parra-Olea G, Wake DB. Extreme morphological and ecological homoplasy in tropical salamanders. Proc Natl Acad Sci U S A. 2001:98:7888–7891. https://doi.org/10.1073/pnas.131203598.

Pirani RM, et al. A high-quality genome for the slender anole (*Anolis apletophallus*): an emerging model for field studies of tropical ecology and evolution. G3 (Bethesda). 2023:14:jkad248. https://doi.org/10.1093/g3journal/jkad248.

Downloaded from https://academic.oup.com/gbe/article/17/11/evaf196/8303492 by guest on 27 January 2026

Poe S, et al. A phylogenetic, biogeographic, and taxonomic study of all extant species of *Anolis* (Squamata; Iguanidae). Syst Biol. 2017:66: 663–697. https://doi.org/10.1093/sysbio/syx029.
Pörtner H. Climate change and temperature-dependent biogeography: oxygen limitation of thermal tolerance in animals. Naturwissenschaften. 2001:88:137–146. https://doi.org/10.1007/s001140100216.
Putnam NH, et al. Chromosome-scale shotgun assembly using an in vitro method for long-range linkage. Genome Res. 2016:26: 342–350. https://doi.org/10.1101/gr.193474.115.
QGIS.org. QGIS Geographic Information System. 2020. http://www.qgis.org. Accessed 2022 January 14.
R Core Team. R: A language and environment for statistical computing. 2022. https://www.R-project.org/. Accessed 2021 December 23.
Ríos-Orjuela JC, Camacho-Bastidas JS, Jerez A. Appendicular morphology and locomotor performance of two morphotypes of continental anoles: *Anolis heterodermus* and *Anolis tolimensis*. J Anat. 2020:236:252–273. https://doi.org/10.1111/joa.13092.
Ritzman TB, et al. The gross anatomy of the original and regenerated tail in the green anole (*Anolis carolinensis*). Anat Rec. 2012:295: 1596–1608. https://doi.org/10.1002/ar.22524.
Rivadeneira F, et al. Twenty bone-mineral-density loci identified by large-scale meta-analysis of genome-wide association studies. Nat Genet. 2009:41:1199–1206. https://doi.org/10.1038/ng.446.
Rodríguez A, et al. Genomic and phenotypic signatures of climate adaptation in an *Anolis* lizard. Ecol Evol. 2017:7:6390–6403. https://doi.org/10.1002/ece3.2985.
Rossi M, et al. Dissecting the mechanisms of bone loss in Gorham-Stout disease. Bone. 2020:130:115068. https://doi.org/10.1016/j.bone.2019.115068.
Rotwein P. Insulinlike growth factor 1 gene variation in vertebrates. Endocrinology. 2018:159:2288–2305. https://doi.org/10.1210/en.2018-00259.
Rovatsos M, Altmanová M, Pokorná M, Kratochvíl L. Conserved sex chromosomes across adaptively radiated *Anolis* lizards: brief communication. Evolution. 2014:68:2079–2085. https://doi.org/10.1111/evo.12357.
Rubin C-J, et al. Rapid adaptive radiation of Darwin's finches depends on ancestral genetic modules. Sci Adv. 2022:8:eabm5982. https://doi.org/10.1126/sciadv.abm5982.
Sakamoto F, et al. Detection of evolutionary conserved and accelerated genomic regions related to adaptation to thermal niches in *Anolis* lizards. Ecol Evol. 2024:14:e11117. https://doi.org/10.1002/ece3.11117.
Schluter D. The ecology of adaptative radiation. Oxford University Press; 2000.
Schneider CA, Rasband WS, Eliceiri KW. NIH image to ImageJ: 25 years of image analysis. Nat Methods. 2012:9:671–675. https://doi.org/10.1038/nmeth.2089.
Schrader L, Schmitz J. The impact of transposable elements in adaptive evolution. Mol Ecol. 2019:28:1537–1549. https://doi.org/10.1111/mec.14794.
Seebacher F, Murray SA, Else PL. Thermal acclimation and regulation of metabolism in a reptile (*Crocodylus porosus*): the importance of transcriptional mechanisms and membrane composition. Physiol Biochem Zool. 2009:82:766–775. https://doi.org/10.1086/605955.
Seehausen O, et al. Genomics and the origin of species. Nat Rev Genet. 2014:15:176–192. https://doi.org/10.1038/nrg3644.
Seixas FA, Edelman NB, Mallet J. Synteny-based genome assembly for 16 species of *Heliconius* butterflies, and an assessment of structural variation across the genus. Genome Biol Evol. 2021:13: evab069. https://doi.org/10.1093/gbe/evab069.
Shiels H, et al. TRAF4 deficiency leads to tracheal malformation with resulting alterations in air flow to the lungs. Am J Pathol. 2000:157: 679–688. https://doi.org/10.1016/s0002-9440(10)64578-6.
Shindo T, et al. Regulation of cardiovascular development and homeostasis by the adrenomedullin-RAMP system. Peptides. 2019:111: 55–61. https://doi.org/10.1016/j.peptides.2018.04.004.
Shiraishi S, et al. S-myotrophin promotes the hypertrophy of skeletal muscle of mice in vivo. Int J Biochem Cell Biol. 2006:38: 1114–1122. https://doi.org/10.1016/j.biocel.2005.11.014.
Shu B, et al. BMP2, but not BMP4, is crucial for chondrocyte proliferation and maturation during endochondral bone development. J Cell Sci. 2011:124:3428–3440. https://doi.org/10.1242/jcs.083659.
Silva FA, Souza ÉMS, Ramos E, Freitas L, Nery MF. The molecular evolution of genes previously associated with large sizes reveals possible pathways to cetacean gigantism. Sci Rep. 2023:13:67. https://doi.org/10.1038/s41598-022-24529-3.
Simão FA, Waterhouse RM, Ioannidis P, Kriventseva EV, Zdobnov EM. BUSCO: assessing genome assembly and annotation completeness with single-copy orthologs. Bioinformatics. 2015:31:3210–3212. https://doi.org/10.1093/bioinformatics/btv351.
Smit AFA, Hubley R, Green P. RepeatMasker. 2015. http://www.repeatmasker.org. Accessed 2021 April 1.
Soccio RE, et al. The cholesterol-regulated StarD4 gene encodes a StAR-related lipid transfer protein with two closely related homologues, StarD5 and StarD6. Proc Natl Acad Sci U S A. 2002:99: 6943–6948. https://doi.org/10.1073/pnas.052143799.
Stanke M, et al. AUGUSTUS: ab initio prediction of alternative transcripts. Nucleic Acids Res. 2006:34:W435–W439. https://doi.org/10.1093/nar/gkl200.
Stroud JT, Losos JB. Ecological opportunity and adaptive radiation. Annu Rev Ecol Evol Syst. 2016:47:507–532. https://doi.org/10.1146/annurev-ecolsys-121415-032254.
Sun B, et al. Higher metabolic plasticity in temperate compared to tropical lizards suggests increased resilience to climate change. Ecol Monogr. 2022:92:e1512. https://doi.org/10.1002/ecm.1512.
Supek F, Bošnjak M, Škunca N, Šmuc T. REVIGO summarizes and visualizes long lists of gene ontology terms. PLoS One. 2011:6:e21800. https://doi.org/10.1371/journal.pone.0021800.
Szklarczyk D, et al. STRING v11: protein–protein association networks with increased coverage, supporting functional discovery in genome-wide experimental datasets. Nucleic Acids Res. 2019:47: D607–D613. https://doi.org/10.1093/nar/gky1131.
Tejedor G, et al. Whole embryo culture, transcriptomics and RNA interference identify TBX1 and FGF11 as novel regulators of limb development in the mouse. Sci Rep. 2020:10:3597. https://doi.org/10.1038/s41598-020-60217-w.
Tollis M, et al. Comparative genomics reveals accelerated evolution in conserved pathways during the diversification of anole lizards. Genome Biol Evol. 2018:10:489–506. https://doi.org/10.1093/gbe/evy013.
Velasco JA, et al. Climatic niche attributes and diversification in *Anolis* lizards. J Biogeogr. 2016:43:134–144. https://doi.org/10.1111/jbi.12627.
Vouyovitch CM, et al. WNT4 mediates the autocrine effects of growth hormone in mammary carcinoma cells. Endocr Relat Cancer. 2016:23:571–585. https://doi.org/10.1530/erc-15-0528.
Wagner G, et al. LMO3 reprograms visceral adipocyte metabolism during obesity. J Mol Med. 2021:99:1151–1171. https://doi.org/10.1007/s00109-021-02089-9.
Wang RN, et al. Bone morphogenetic protein (BMP) signaling in development and human diseases. Genes Dis. 2014:1:87–105. https://doi.org/10.1016/j.gendis.2014.07.005.
Wang Y, et al. Loss of CIB2 causes profound hearing loss and abolishes mechanoelectrical transduction in mice. Front Mol Neurosci. 2017:10:401. https://doi.org/10.3389/fnmol.2017.00401.
Ward AB, Mehta RS. Axial elongation in fishes: using morphological approaches to elucidate developmental mechanisms in studying

Downloaded from https://academic.oup.com/gbe/article/17/11/evaf196/8303492 by guest on 27 January 2026

body shape. Integr Comp Biol. 2010:50:1106–1119. https://doi.org/10.1093/icb/icq029.
Wellborn GA, Langerhans RB. Ecological opportunity and the adaptive diversification of lineages. Ecol Evol. 2015:5:176–195. https://doi.org/10.1002/ece3.1347.
Wogan GOU, Yuan ML, Mahler DL, Wang IJ. Hybridization and transgressive evolution generate diversity in an adaptive radiation of *Anolis* lizards. Syst Biol. 2023:72:874–884. https://doi.org/10.1093/sysbio/syad026.
Wollenberg Valero KC, et al. A candidate multimodal functional genetic network for thermal adaptation. PeerJ. 2014:2:e578. https://doi.org/10.7717/peerj.578.
Ye Z, Kimelman D. *Hox13* genes are required for mesoderm formation and axis elongation during early zebrafish development. Development. 2020:147:dev185298. https://doi.org/10.1242/dev.185298.
Zecchini S, et al. Autophagy controls neonatal myogenesis by regulating the GH-IGF1 system through a NFE2L2- and DDIT3-mediated mechanism. Autophagy. 2019:15:58–77. https://doi.org/10.1080/15548627.2018.1507439.
Zhang Q, et al. Roles and action mechanisms of WNT4 in cell differentiation and human diseases: a review. Cell Death Discov. 2021a:7:287. https://doi.org/10.1038/s41420-021-00668-w.
Zhang Y, et al. S100a gene family: immune-related prognostic biomarkers and therapeutic targets for low-grade glioma. Aging (Albany NY). 2021b:13:15459–15478. https://doi.org/10.18632/aging.203103.
Zheng Q-W, et al. PPDPF promotes lung adenocarcinoma progression via inhibiting apoptosis and NK cell-mediated cytotoxicity through STAT3. Oncogene. 2022:41:4244–4256. https://doi.org/10.1038/s41388-022-02418-3.
Zhu J, et al. Phosphorylation of PLIN3 by AMPK promotes dispersion of lipid droplets during starvation. Protein Cell. 2019:10:382–387. https://doi.org/10.1007/s13238-018-0593-9.
Zhu S, et al. Calmodulin interacts with Rab3D and modulates osteoclastic bone resorption. Sci Rep. 2016:6:37963. https://doi.org/10.1038/srep37963.

Associate editor: Diego Cortez

Downloaded from https://academic.oup.com/gbe/article/17/11/evaf196/8303492 by guest on 27 January 2026